Typeset with jjap2.cls <ver.1.0> **Regular Paper**

Picosecond Ultrasound Spectroscopy with a Stable Fiber Laser for Ultrahigh-Frequency-Oscillator Applications: from Nanomechanics to Biosensors

Hirotsugu Ogi, Tetsuya Kawamoto, Yohei Nakamichi and Masahiko Hirao

Graduate School of Engineering Science, Osaka University, Toyonaka, Osaka 560-8531, Japan

We developed a stable picosecond-ultrasound-spectroscopy system with a fiber-laser light source. A linearly polarized light pulse with 532 nm wavelength is split into pump and probe light pulses using a polarized beam splitter (PBS). The ultrahigh-frequency acoustic waves excited by the pump light pulse are successfully detected using the delayed probe light pulse with a signal-to-noise ratio higher than that of the traditional titanium-sapphire pulse laser. The wavelength used allows deep inspection of silicon because of less light absorption. The developed system is also applied to a biosensor with an ultrathin Pt film resonator, which shows significantly improved stability at 100 GHz. The amount of frequency change caused by the adsorption of target molecules is of the order of 10^{-2}, which is much higher than that detected with conventional oscillator biosensors by a factor of 10^4.

1. Introduction

Irradiation of nanostructure materials (ultrathin films, nanowires, and nanodots) with ultrafast light pulses generates ultrahigh-frequency acoustic waves or Γ-point vibrations of the nanostructures,[1)] which can be detected using a time-delayed ultrafast probe light pulse through changes in its reflectivity. This phenomenon was first observed by Thomsen and coworkers,[2,3)] and several pioneers developed methods for studying ultrahigh-frequency coherent phonons and mechanics of nanoscale materials, establishing a new field of study, the so-called picosecond ultrasonics. Their contributions include improvement of optics,[4)] studies on surface-wave propagations,[5)] ultrasonic attenuation at high frequencies,[6–8)] diffusion of carriers in semiconductors,[9)] thermal excitation of shear waves,[10–12)] elastic constants of ultrathin films,[13–18)] and vibrations related to patterned nanostructures.[19–23)]

Picosecond ultrasonics thus continues to receive intensive attention because it is a powerful tool for nanomechanics. In previous studies, a titanium-sapphire (Ti/S) pulse laser with a wavelength near 800 nm is used, because it provides significantly high-power (>∼1 W) and short-duration (<∼200 fs) light pulses. However, because the change in the reflectivity of the probe light pulse owing to acoustic strain is very small, lock-in-amplifier detection has been adopted for the intensity modulation of the pump light pulse. This required complete blocking of scattered pump lights, which do not irradiate the specimen and cause strong background noise, to the photoreceiver. Therefore, different wavelengths have been used for

pump and probe lights so as to block pump lights using color filters, and a high enough power was required to obtain the frequency-doubled light pulse with a second-harmonic-generator crystal. The high-power Ti/S pulse laser is suitable for meeting this requirement. However, there are two disadvantages in using a Ti/S pulse laser. First, the optics for the mode-locked-laser cavity occupies a large space, and the entire measurement system can never be compact, which typically requires a space of 2x2 m^2. Second, the intensity of the Ti/S pulse laser is unstable. One of the important applications of picosecond ultrasonics is ultrahigh-frequency oscillator biosensor,[24,25] where acoustic responses at resonance of an ultrathin film are monitored during the binding reaction between biomolecules. Because the binding reaction takes a long time (∼30 min), a stable baseline is needed. However, the output intensity of a Ti/S pulse laser fluctuates by 1-5% for 1 h. Considering that the baseline fluctuation of a conventional quartz-crystal-microbalance biosensor is smaller than 1 ppm,[26,27] this unstable operation of the Ti/S pulse laser must be improved for biosensor applications.

In this study, we propose the picosecond ultrasonic spectroscopy with a stable fiber laser instead of the Ti/S pulse laser. A mode-locked fiber laser shows a large gain bandwidth of rare-earth-doped fibers and high stability over a long-time operation (intensity fluctuation is less than 0.1% for 1 h), and consists of very compact apparatuses. (The area for the entire system, including the free-space optics, is only one-third of that with a Ti/S pulse laser.) Therefore, the disadvantages with the Ti/S pulse laser will be solved. However, the peak power of the light pulse markedly decreases at wavelengths below 1 μm owing to strong nonlinearities of fibers. For examining metallic materials, a shorter wavelength is suitable both for the pump and probe lights because of two reasons. First, the reflection coefficient of the light energy increases as wavelength increases. For example, if we use the light pulse with 1064 nm wavelength as the pump light, 97% of the energy is reflected at the Cu surface, and only 3% of the energy of the pump light pulse can be used for the acoustic-wave generation. However, the reflection coefficient decreases at 532 nm (61%). Second, the detection sensitivity of the probe light pulse to the elastic strain is governed by the piezo-optic constants of the material, which are significantly small for wavelengths longer than 800 nm.[28,29] Therefore, the fiber laser was not adopted in picosecond ultrasonic systems in the past because it generates only low-energy visible lights, which cannot generate the frequency-doubled light pulse with a sufficient power.

We then develop optics for splitting the light pulse into two pulses by polarization, not by the wavelength with retention of their sufficiently high power. We apply our measurement system to the study of vibrations in an ultrathin Pt film, an amorphous SiO_2 film on a Si substrate, a Pt/silicon-nitride free-standing film, and to a biosensor with an ultrathin Pt film. We demonstrate the higher capability of picosecond ultrasonics with fiber lasers.

2. Experimental Procedure

2.1 Optics

Figure 1 shows the optics for the picosecond ultrasonic system with the fiber laser. The linearly polarized light pulse at the output has a wavelength of 1064 nm, a pulse duration of 150 fs and a pulse repetition rate of 50 MHz. Because this wavelength is too large and inappropriate for picosecond ultrasonics, we focus it on a second-harmonic-generator crystal to obtain a visible 532 nm light pulse with a 100 mW power. The light pulse propagates through a $\lambda/2$ wavelength plate, which rotates the polarization direction. The pump and probe light pulses are separated by a polarizing beam splitter (PBS). The optical length of the pump light pulse with the perpendicular polarization is controlled by a mobile stage controller, thus producing a difference in optical length between the pump and probe lights. The intensity of pump light pulses is modulated at 1 MHz by an acousto-optic modulator. They are reflected by the other PBS and irradiate the specimen perpendicularly to the surface, which generate ultrahigh-frequency vibrations through thermal expansion and shrinking. The time-delayed probe light pulses with the in-plane polarization pass through the PBS crystals and irradiate the specimen perpendicularly to the surface to detect the oscillation phenomena in the specimen through the photoelasic effect. The reflected probe light pulses pass through the PBS near the specimen and enter the balance photodetector. The baseline-subtracted output from the detector enters a lock-in amplifier, which extracts the modulation-frequency components, providing information on the vibrations inside the specimen.

2.2 Specimens

We used three specimens. The first specimen was an ultrathin Pt film deposited on a borosilicate-glass substrate. The magnetron-sputtering method was used to prepare the specimen, and the film thickness was determined to be 20.3 nm by x-ray total-reflectivity measurement.[13,30] The second specimen was an amorphous SiO_2 thin film deposited on a (001) Si substrate by a DC sputtering method.[16] A 10 nm Al film was deposited on the top surface for the acoustic-wave generator. The third specimen was a Pt/Si_3N_4 free-standing film on the Si substrate. A 94.5 nm Si_3N_4 film was deposited by the chemical-vapor-deposition method, and the center rectangular part of the Si substrate (2x2 mm^2) was removed by anisotropic etching with a potassium-hydroxide solution to fabricate partially free-standing Si_3N_4 film. The 15 nm Pt film is then deposited on the Si_3N_4 film by the magnetron sputtering method. For this specimen, we contacted water with the Pt surface and irradiated the specimen from the silicon-nitride side with the light pulses to obtain phonon information from the water as well.

2.3 Biosensor application

As demonstrated in our previous studies,[24,25] the picosecond ultrasonic system is highly applicable as an ultrahigh-sensitive oscillator biosensor, because the mass sensitivity of an oscillator biosensor is markedly enhanced as oscillator thickness decreases.[31,32] Considering that the oscillator used in a conventional oscillator biosensor is thicker than 10 μm quartz plates and the picosecond ultrasonic system can vibrate 10-100 nm oscillators, the sensitivity for adsorbed mass on the oscillator is drastically enhanced. However, instability of the laser output intensity caused an instability of the baseline of the acoustic responses during antigen-antibody reactions. We then investigate the applicability of the picosecond ultrasound spectroscopy with the fiber laser to the biosensor using the 15 nm Pt film on the borosilicate-glass substrate. We detected human immunoglobulin G (hIgG) as an antigen with an anti-hIgG antibody as a receptor immobilized on the Pt surface. The preparation method for the Pt film and the surface modification procedure were the same as those used in our previous study.[24]

3. Results

Figure 2(a) shows the time-resolved reflectivity changes of the probe light observed from the 20.3 nm Pt film on the glass substrate using the Ti/S laser optics (800 nm for pumping and 400 nm for probing) and the fiber-laser optics (532 nm for the pump and probe lights). A single scan of the delay line was adopted in both measurements. We observe high-frequency vibrations at 100 GHz in both experiments.

Figure 2(b) shows a comparison of reflectivity changes for the amorphous SiO_2 film on the Si substrate measured using the Ti/S laser system with those measured using the fiber-laser system. Low-frequency and high-frequency Brillouin oscillations (BOs) are observed in both experiments, which correspond to BO from the SiO_2 film and that from Si substrate, respectively. The attenuation of BO in Si is small in the case of using the fiber laser.

Figure 3(a) shows the reflectivity change of the Pt/Si_3N_4 free-standing film measured using the fiber-laser system. Small-attenuation vibration continues in this case, consisting of three frequency components of 7.25, 34.3, and 82.1 GHz, as shown in Fig. 3(b).

Figure 4(a) shows the changes in the vibrational amplitude of the Pt film at a fixed time of 30 ps during the antigen-antibody reaction. The corrected data for the drifting baseline shift during the steady flow of a phosphate-buffered-saline solution are also given. The arrival of the hIgG solution (antigen) caused the change in the amplitude, and a part of the decrement was recovered by the injection of glycine HCl buffer solution (GHB). Figure 4(b) show the reflectivity changes before and after the injection of the hIgG solution. As shown in Figs. 4(c) and 4(d), the resonance frequency of the Pt film decreased by 1.7% after the binding reaction.

4. Discussion

4.1 Nanomechanics application

The resonance frequency of the vibration in Fig. 2(a) is 100 GHz, which agrees with the longitudinal-wave resonance frequency in a (111) textured Pt with both free ends: Because the closed-packed plane of Pt, the (111) plane, tends to be parallel to the surface during the deposition, the highly (111) textured structure is often observed in a Pt film.[13] Thus, taking 384.5 GPa for the longitudinal-wave modulus along the $\langle 111 \rangle$ direction,[13] the fundamental resonance frequency is calculated to be 104 GHz. The slightly lower observation frequency is acceptable because of imperfection of the (111) texture and defects in the film, lowering the macroscopic stiffness. The fiber laser provided a better S/N ratio, as seen in Fig. 2(a). One reason will be a larger transmission coefficient of the pump light into the Pt film at 532 nm (37%) than at 800 nm (29%). Also, a more stable output with the fiber laser will contribute to the higher S/N ratio.

The oscillations observed in Fig. 2(b) are BOs, which appear because of interference between the surface-reflected probe light and backwardly diffracted probe light inside the material by the propagating acoustic strain.[7,16] The longitudinal wave generated in the surface ultrathin Al by the pump light pulse propagates in the depth direction, causing the backward diffraction of the probe light pulse. The lower frequency oscillation appears just after the excitation, which is BO from SiO_2 film. The following high-frequency oscillation is BO from the Si substrate. The BO frequency f_{BO} is determined by $f_{BO} = 2nv/\lambda$, where n, v, and λ denote the refractive index, the sound velocity of the material, and the wavelength of the probe light, respectively. Using literature values, we predict f_{BO} values to be 43.5 and 33.2 GHz in amorphous SiO_2 at 400 and 532 nm, respectively, and 235 and 132 GHz in (001) Si at 400 and 532 nm, respectively. These predictions are in good agreement with experimental values; f_{BO} values in the SiO_2 film are 45.0 and 33.1 GHz at 400 and 532 nm, respectively, and f_{BO} values in the Si substrate are 235.4 and 131.4 GHz at 400 and 532 nm, respectively. Thus, measuring BO frequencies accurately allows us to determine sound velocity and then the elastic constants of thin films and substrates without thickness information. A more important observation in Fig. 2(b) is that BO in the Si substrate lasts longer with the fiber laser than with the Ti/S laser. It is observed from 150 to 350 ps using the 532 nm probe light, corresponding to the perpetration from the surface to about 1.7 μm. This depth, however, decreases to be about 300 nm in the case of using the 400 nm probe light because of a more significant adsorption; the values of the imaginary part of the refractive index ($-k$ value) in Si are 0.043 at 532 nm and 0.387 at 400 nm. Therefore, we can evaluate mechanical properties and defect information of Si in deeper regions using the fiber-laser optics.

Figure 3(a) indicates the mechanical vibration of the double-layer free-standing film consisting of 15 nm Pt and 94.5 nm Si_3N_4. We have derived the frequency equation for a mul-

tilayer film,[33] and using reported longitudinal-wave velocities and mass densities of Pt[13] and Si_3N_4,[34] we calculated the resonance frequencies of the double-layer film to be 34.3 and 82.1 GHz for the fundamental and second modes, respectively. These predicted values show excellent agreements with the measurement values shown in Fig. 3(b), indicating that we can determine the sound velocities of individual layers inversely by fitting the theoretically determined frequencies to the measurement values. Furthermore, we see a low-frequency peak near 7 GHz in Fig. 3(b). Because this peak disappears when the water is not in contact with the Pt film, we consider that BO in water is observed when using this system. The high-frequency acoustic phonons generated in the Pt film propagated into the water, which caused the backward diffraction of the probe light pulse reaching the water region. Indeed, the theoretical value of f_{BO} in water at 532 nm is 7.53 GHz, showing good agreement with the measurement value (7.25 GHz).

4.2 Biosensor application

Figure 4(a) shows the great capability of this system for biosensor applications. A 10 ng/ml hIgG is successfully detected by monitoring vibrational amplitude, which is difficult to detect with a conventional oscillator biosensor owing to the low concentration of hIgG. For example, Natesan et al.[35] used a relatively high-frequency (16.5 MHz) quartz-crystal microbalance biosensor for detecting staphylococcal enterotoxin B, whose detection limit was about 25 ng/ml. Although the baseline drift sometimes appeared, which may be caused by the drift of the specimen owing to the solution flow, the baseline stability is considerably improved with the fiber laser; the baseline fluctuation became smaller than that with the Ti/S laser by a factor of 0.1. Moreover, the frequency decrease can be observed, as shown in Figs. 4(b)-4(d). Such a clear frequency change was not observed with the Ti/S-laser optics for a Pt film biosensor because of unstable acoustic responses.[24,25] The amount of frequency change due to the adsorption of the antigen reaches 1.7%, which is much larger than that detected with previous oscillator biosensors using quartz resonators by a factor of 10^4. (The frequency change was about 0.0007% for detecting a 100 ng/ml hIgG even with a highly sensitive quartz-crystal-microbalance biosensor.[36])

5. Conclusions

We have successfully developed a picosecond ultrasound spectroscopy system with a stable fiber laser. The pump and probe light pulses are distinguished by their polarization direction, having the same wavelength of 532 nm. The newly developed system was applied to ultrathin films, a multilayer thin film, and an amorphous silica thin film on a silicon substrate. The ultrahigh-frequency vibrations and Brillouin oscillations were detected with a S/N ratio higher than that obtained with a previous Ti/S pulse laser system. Concerning Si, the 532 nm probe light showed better inspection capability because of less adsorption of light. Our system was

then applied to a biosensor field and showed more stable acoustic responses. It clearly detected 10 ng/ml hIgG through its reaction with anti-hIgG antibody immobilized on the 15 nm Pt oscillator film. The frequency decrease of 1.7% was observed after the binding reaction due to the mass loading.

References

1) H. Tanei, K. Kusakabe, H. Ogi, N. Nakamura, and M. Hirao: Appl. Phys. Lett. **95** (2009) 011902.
2) C. Thomsen, J. Strait, Z. Vardeny, H. J. Maris, and J. Tauc: Phys. Rev. Lett. **53** (1984) 989.
3) C. Thomsen, H.T. Grahn, H.J. Maris, and J. Tauc: Phys. Rev. B **34** (1986) 4129.
4) D. H. Hurley and O. B. Wright: Opt. Lett. **24** (1999) 1305.
5) Y. Sugawara, O. B. Wright, O. Matsuda, M. Takigahira, Y. Tanaka, S. Tamura, and V. E. Gusev: Phys. Rev. Lett. **88** (2002) 185504.
6) T. C. Zhu, H. J. Maris, and J. Tauc: Phys. Rev. B **44** (1991) 4281.
7) P. Emery and A. Devos: Appl. Phys. Lett. **89** (2006) 191904.
8) S. Ayrinhac, M. Foret, A. Devos, B. Ruffle, E. Courtens, and R. Vacher: Phys. Rev. B **83** (2011) 014204.
9) O. B. Wright, B. Perrin, O. Matsuda, and V. E. Gusev: Phys. Rev. B **64** (2001) 081202.
10) O. Matsuda, O. B. Wright, D. H. Hurley, V. E. Gusev, and K. Shimizu: Phys. Rev. Lett. **93** (2004) 095501.
11) T. Pezeril, P. Ruello, S. Gougeon, N. Chigarev, D. Mounier, J.-M. Breteau, P. Picart, and V. Gusev: Phys. Rev. B **75** (2007) 174307.
12) O. Matsuda, O. B. Wright, D. H. Hurley, V. Gusev, and K. Shimizu: Phys. Rev. B **77** (2008) 224110.
13) H. Ogi, M. Fujii, N. Nakamura, T. Yasui, and M. Hirao: Phys. Rev. Lett. **98** (2007) 195503.
14) H. Ogi, M. Fujii, N. Nakamura, T. Shagawa, and M. Hirao: Appl. Phys. Lett. **90** (2007) 191906.
15) N. Nakamura, H. Ogi, T. Yasui, M. Fujii, and M. Hirao: Phys. Rev. Lett. **99** (2007) 035502.
16) H. Ogi, T. Shagawa, N. Nakamura, M. Hirao, H. Odaka, and N. Kihara: Phys. Rev. B **78** (2008) 134204.
17) K. Tanigaki, T. Kusumoto, H. Ogi, N. Nakamura, and M. Hirao: Jpn. J. Appl. Phys. **49** (2010) 07HB01.
18) N. Nakamura, A. Uranishi, M. Wakita, H. Ogi, and M. Hirao: Jpn. J. Appl. Phys. **49** (2010) 07HB04.
19) H.-N. Lin, H. J. Maris, L. B. Freund, K. Y. Lee, H. Luhn, and D. P. Kern: J. Appl. Phys. **73** (1993) 37.
20) G. A. Antonelli, H. J. Maris, S. G. Malhotra, and J. M. E. Harper: J. Appl. Phys. **91** (2002) 3261.

21) J.-F. Robillard, A. Devos, and I. Roch-Jeune: Phys. Rev. B **76** (2007) 092301.

22) J.-F. Robillard, A. Devos, I. Roch-Jeune, and P. Mante: Phys. Rev. B **78** (2008) 064302.

23) H. Ogi, A. Yamamoto, K. Kondou, K. Nakano, K. Morita, N. Nakamura, T. Ono, and M. Hirao: Phys. Rev. B **82** (2010) 155436.

24) H. Ogi, K. Matsumoto, Y. Fujita, T. Kawamoto, N. Nakamura, and M. Hirao: Appl. Phys. Express **3** (2010) 017001.

25) H. Ogi, T. Kawamoto, N. Nakamura, M. Hirao, and M. Nishiyama: Biosen. Bioelectron. **26** (2010) 1273.

26) M. Rodahl and B. Kasemo: Sens. Actuators A **54** (1996) 448.

27) E. Nilebäck, L. Feuz, H. Uddenberg, R. Valiokas, and S. Svedhem: Biosen. Bioelectron. **28** (2011) 407.

28) U. Gerhardt: Phys. Rev. **172** (1968) 651.

29) P. Etchegoin, J. Kircher, and M. Cardona: Phys. Rev. B **47** (1993) 10292.

30) L. Parratt: Phys. Rev. **95** (1954) 359.

31) H. Ogi, H. Nagai, Y. Fukunishi, M. Hirao, and M. Nishiyama: Anal. Chem. **81** (2009) 8068.

32) F. Kato, H. Ogi, T. Yanagida, S. Nishikawa, M. Nishiyama, and M. Hirao: Jpn. J. Appl. Phys. **50** (2011) 07HD03.

33) H. Ogi, Y. Fukunishi, T. Omori, K. Hatanaka, M. Hirao, and M. Nishiyama: Anal. Chem. **80** (2008) 5494.

34) K. J. Singh, Y. Matsuda, K. Hattori, H. Nakano, and S. Nagai: Ultrasonics **41**(2003) 9.

35) M. Natesan, M. A. Cooper, J. P. Tran, V. R. Rivera, and M. A. Poli: Anal. Chem. **81** (2009) 3896.

36) H. Ogi, K. Motohisa, K. Hatanaka, T. Ohmori, M. Hirao, and M. Nishiyama: Biosens. Bioelectron. **22** (2007) 3238.

Figure Captions

Fig. 1 (a) Optics for the picosecond ultrasound spectroscopy with the fiber laser. The power on the specimen surface is 3 mW both for pump and probe lights.

Fig. 2 Reflectivity changes (ΔR) observed using the Ti/S-laser optics and the fiber-laser optics for (a) 20.3 nm Pt on the glass substrate and (b) 920 nm amorphous SiO_2 on (001) Si substrate.

Fig. 3 (a) Reflectivity changes (ΔR) from the 15 nm Pt/94.5 nm Si_3N_4 free-standing double-layer film observed using the fiber-laser optics, and (b) its Fourier spectrum. The broken vertical lines are theoretically calculated resonance frequencies of the double layer.

Fig. 4 (Color online)(a) Changes in the vibrational amplitude of 15 nm Pt on the glass substrate at 30 ps during the binding reaction between hIgG and anti-hIgG antibody immobilized on the Pt surface. The correction data for the baseline drifting (inclined broken lines) is shown by the red line. (b) Changes in the vibration behavior of the Pt film before and after the injection of the hIgG solution and (c) their Fourier spectrum. (d) Changes in the resonance frequency of the Pt film before and after the binding reaction.

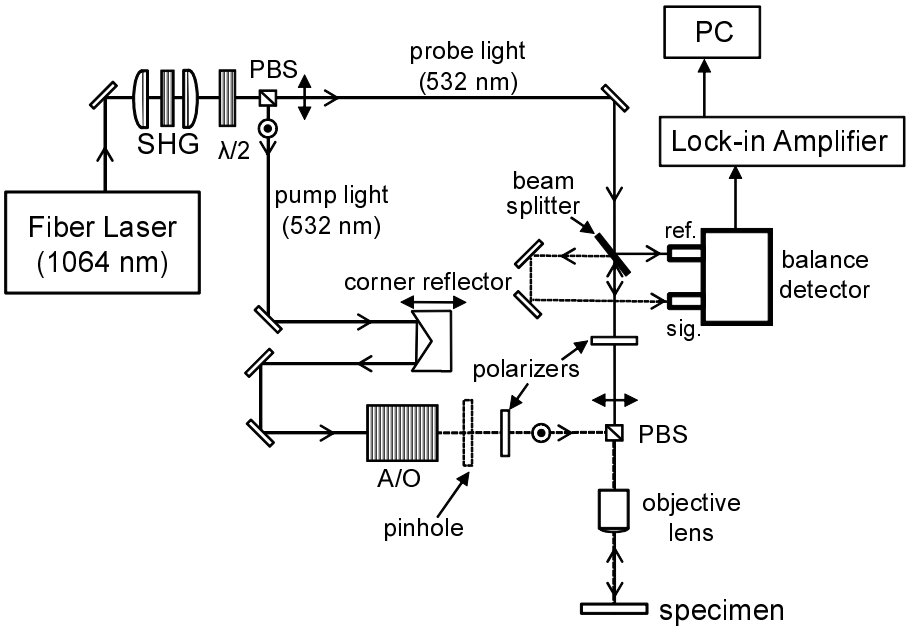
PC
Lock-in Amplifier
probe light
(532 nm)
PBS
SHG
λ/2
Fiber Laser
(1064 nm)
pump light
(532 nm)
beam
splitter
ref.
balance
detector
sig.
corner reflector
polarizers
PBS
A/O
pinhole
objective
lens
specimen

Fig. 1.

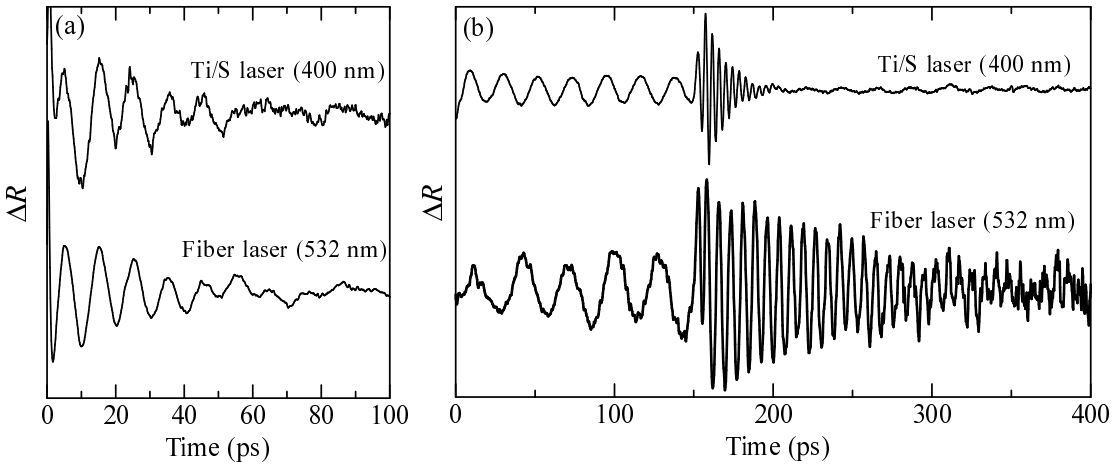
(a)
Ti/S laser (400 nm)
Fiber laser (532 nm)
ΔR
0
20
40
60
80
100
Time (ps)
(b)
Ti/S laser (400 nm)
Fiber laser (532 nm)
ΔR
0
100
200
300
400
Time (ps)

Fig. 2.

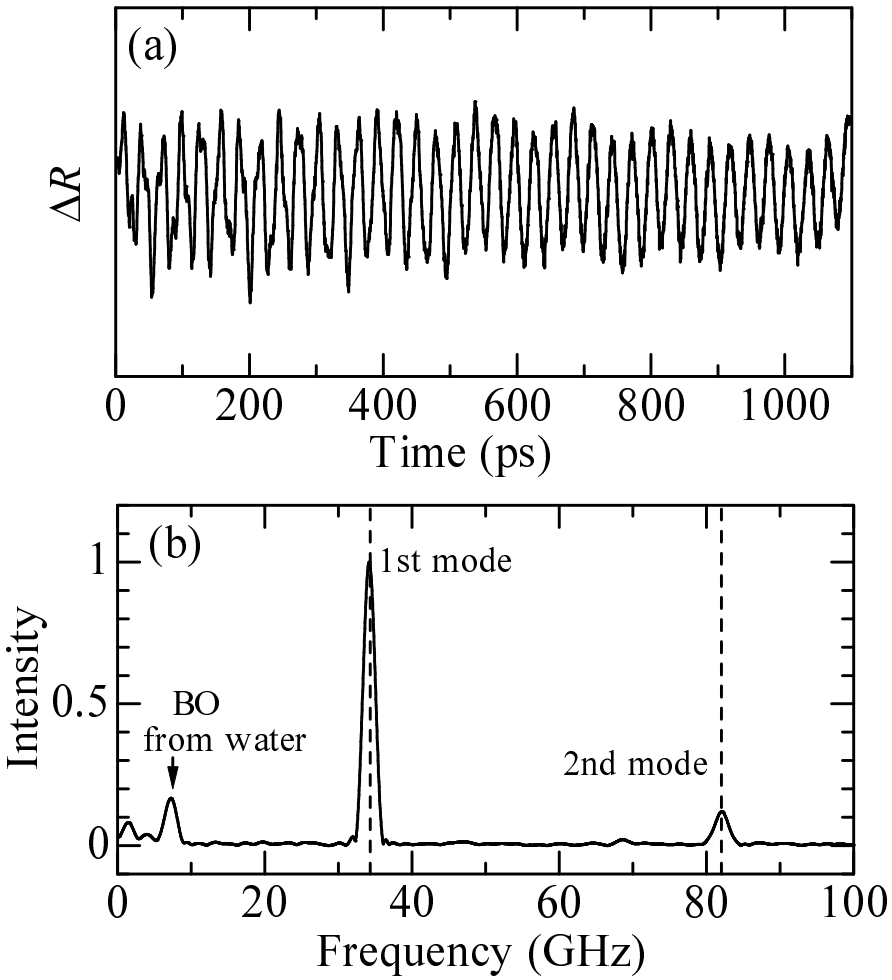
(a)
ΔR
0
200
400
600
800
1000
Time (ps)
(b)
1st mode
BO
from water
2nd mode
Intensity
1
0.5
0
0
20
40
60
80
100
Frequency (GHz)

Fig. 3.

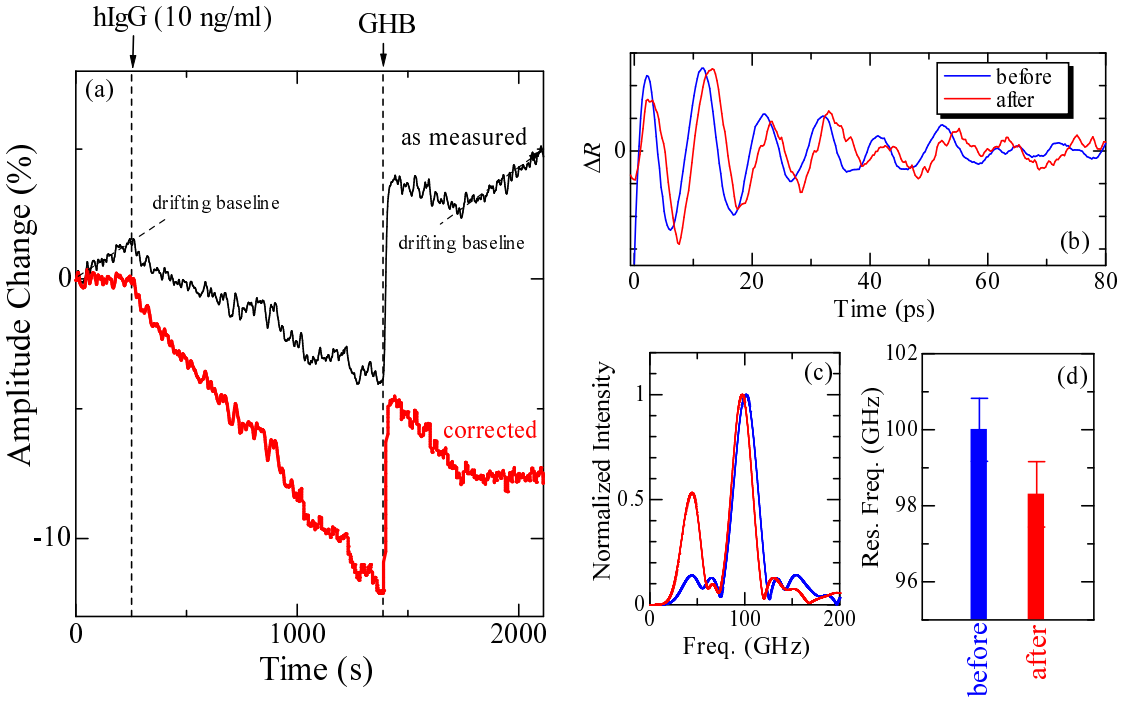
hIgG (10 ng/ml)
GHB
(a)
as measured
drifting baseline
drifting baseline
corrected
Amplitude Change (%)
0
-10
0
1000
2000
Time (s)
ΔR
0
before
after
(b)
0
20
40
60
80
Time (ps)
Normalized Intensity
(c)
1
0.5
0
0
100
200
Freq. (GHz)
Res. Freq. (GHz)
102
100
98
96
(d)
before
after

Fig. 4.